International Journal of Thermophysics, Vol. 25, No. 5, September 2004 (© 2004)

Thermal Conductivity of Chalcogenide As_2S_3 Thin Films[1]

S. W. Kim,[2,3] H. Yu,[2] C. H. Kang,[2] S. H. Lee,[4] and J. C. Kim[4]

In order to investigate the photo-induced thermal property changes in chalcogenide thin films, amorphous As_2S_3 thin film samples, whose thicknesses are 0.5, 1.0, 2.0, and 4.0 μm, were prepared on silicon wafers by thermal evaporation. Their thermal conductivity was measured by the 3ω method between room temperature and 100 °C. These measurements were repeated after the illumination of an Ar^+ laser beam whose photon energy is consistent with the bandgap energy of As_2S_3, and repeated again for annealed films at 180 °C for 1 h. The result shows that the thermal conductivities of fresh films were 0.14 to 0.27 $W \cdot m^{-1} \cdot K^{-1}$; however, the values increase to 0.28–0.47 $W \cdot m^{-1} \cdot K^{-1}$ after illumination of the sample and decrease to 0.19–0.42 $W \cdot m^{-1} \cdot K^{-1}$ after annealing of the sample. These changes can be explained by the change in microstructure produced from the photo-darkening and thermal annealing.

KEY WORDS: arsenic trisulfide; chalcogenide; photo-darkening; thermal conductivity; thin film; three omega method.

1. INTRODUCTION

Non-crystalline chalcogenides are solids without long-range order and, as a consequence, they are intrinsically metastable. These materials are susceptible to light-induced changes because they are characterized by intrinsic structural flexibility. Significant changes in the physical properties and structural modifications induced by light have been evidenced in

[1]Paper presented at the Fifteenth Symposium on Thermophysical Properties, June 22–27, 2003, Boulder, Colorado, U.S.A.

[2]Department of Physics, University of Ulsan, Ulsan 680–749, Korea.

[3]To whom correspondence should be addressed. E-mail: sokkim@ulsan.ac.kr

[4]Division of Physical Metrology, Korea Research Institute of Standards and Science, Taejon 305–600, Korea.

0195-928X/04/0900-1505/0

many amorphous chalcogenide films [1–3]. Recent progress in the study of amorphous chalcogenide materials has led to increased attention on an understanding of their structures and various properties at the microscopic level [4, 5].

Photo-darkening, one of the various photo-induced effects that occur in these materials, is produced by the red shift of the optical bandgap [6, 7] and induces a large change in the optical [3], chemical [8], electrical [9], and thermal properties [10], however, compared to other properties, the thermal properties have not been deeply and widely studied until now.

Among many chalcogenide materials, arsenic trisulfide (As_2S_3) is technically important because of its good transparency in the 0.7–11.0 μm wavelength range and excellent resistance against devitrification, moisture, and corrosion [11, 12]. As_2S_3 exhibits a wide variety of photo-induced phenomena that enable it to be used as an optical imaging or storage medium. Recently, it has found application in various electronic devices, including electro-optic information storage devices and optical mass memories [13]. Therefore, an accurate measurement of thermal properties of As_2S_3 is necessary to study the memory density.

After the investigation of the light-induced optical changes of amorphous As_2S_3 thin film samples coated on the slide glass, the same films with several thicknesses, were deposited on silicon wafers by thermal evaporation, and their thermal conductivity was measured by the 3ω method. These measurements were repeated after illumination by an Ar^+ laser beam whose photon energy is consistent with the bandgap energy of As_2S_3 and continued for the annealed films.

The 3ω method, which was used in this study, was developed by Cahill and Pohl [14] in 1987. This technique was developed to measure the thermal conductivity of isotropic bulk materials whose thermal conductivity values are low; therefore, it can be applied to the measurement of the thermal conductivity of low thermal conductivity thin films coated on high thermal conductivity substrates such as silicon wafers [15–17].

2. THEORY

2.1. Photo-darkening of As_2S_3 Thin Films

When an As_2S_3 film is illuminated with bandgap light, the absorption band moves toward longer wavelengths. We call this phenomenon "photo-darkening" because this means stronger absorption of visible light and consequently the illuminated point becomes dark. The degree of this photo-darkening is dependent on the intensity of the light and begins to saturate at a certain intensity.

Several models have been proposed for describing this photo-darkening; of these models, the "defect model" and "double well potential model" seem to be most appropriate. In accordance with the defect model proposed by Street [18], when the amorphous $As_2S_3$is illuminated by the bandgap light, the lone-pair p electron of the S (sulfur)-atom is excited and an exciton is produced as shown in Fig. 1. This exciton is unstable; therefore, it returns to the original states or forms defect pairs such as D^+ and D^-. When these defect pairs form, the S-atom which has an excess positive charge combines with the nearest S-atom and becomes a D^+ defect, and *vice versa*. When these defect pairs are produced, the microstructure changes locally; therefore, the grain size changes and the absorption coefficient and refractive index increase. In order to return to the original stable state which does not have any defects, heat treatment such as annealing at the glass transition temperature is required.

Tanaka [6] suggested the double-well-potential model which treats the bending flexibility of the atoms. The A–A′ transition of atomic configuration shown in Fig. 2 involves implicitly not only a change in the distance between closed shells (A–B) but also a change in bond angle. Such a bending flexibility is strongly correlated with the ionicity of the chemical bond. Basically these two models are the same.

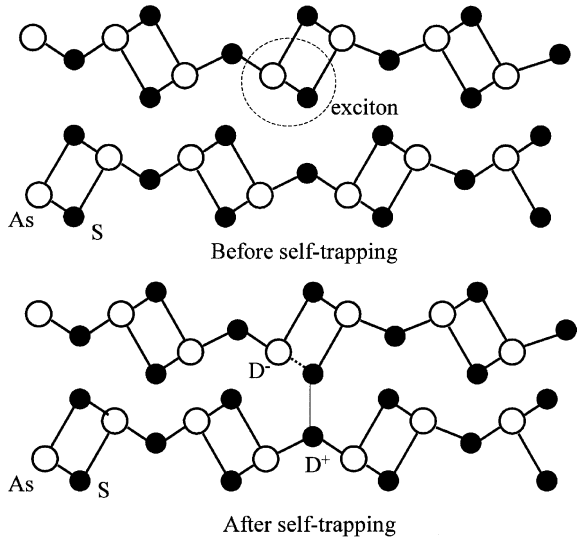

Fig. 1. Schematic of the transformation of an exciton in amorphous As_2S_3into D^+ and D^- pairs accompanied by atomic distortion.

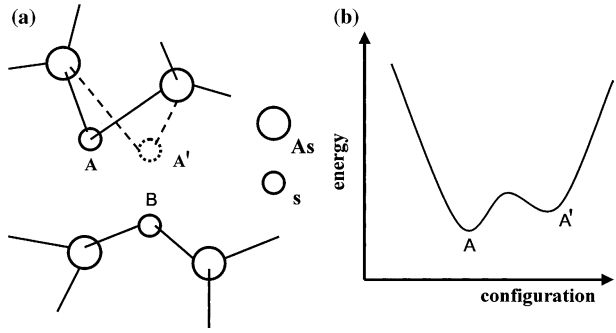

Fig. 2. Schematic model of (a) bistable local bonding geometries and (b) corresponding double-well potential.

2.2. 3ω Method

The sample geometry is shown in Fig. 3. When an ac electric current of angular frequency ω is applied across the heater, it generates Joule heating at 2ω. Two pads are the connections for the current and voltage leads. A gold strip is used simultaneously as the heater and thermometer because it is not susceptible to oxidation and has suitable electrical resistivity. Since the resistance of a pure metal increases with temperature, these temperature oscillations also produce an oscillation of the electrical resistance at a frequency of 2ω. Consequently, the voltage drop across the metal-line has a small component at 3ω that can be used to measure the temperature oscillations and therefore the thermal response of the dielectric film and substrate.

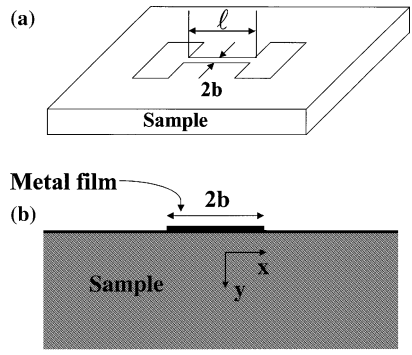

Fig. 3. (a) Shape of prepared sample. The two pads are the connections for current and voltage leads. (b) Geometry of thermal diffusion structure. The full-width of metal line is 2b.

If the amplitude of sinusoidal heating is P, the temperature distribution in the substrate can be calculated as a superposition of temperature modulations by infinitesimal line heaters. The solution given by Carslow and Jaeger [19] for the temperature modulation by a line heater of infinitesimally narrow width is proportional to $K_0(qr)$, where r is the distance from the heater, $K_0(x)$ is the modified Bessel function of zeroth order, and q is defined as [20]

$$q^2 = \frac{2i\omega C}{\kappa}, \tag{1}$$

where C and κ are the heat capacity and thermal conductivity of the sample, respectively. Integrating the solution, by varying the position of infinitesimal heaters over the width of the flat heater, the temperature oscillation amplitude T_{ac} at the heater can be obtained as

$$T_{ac} = \frac{P}{l\pi\kappa} \int_0^\infty \frac{\sin^2(kb)dk}{(kb)^2\sqrt{k^2+q^2.}} \tag{2}$$

The geometrical effect of the metal line as a thermal conductor is neglected in order to express the relation in simpler form. The agreement between calculated and measured T_{ac} shows that this approximation seems to be valid. If the width of the heater is small enough to satisfy the condition $qb \ll 1$, Eq. (2) can be approximated by $\ln(qb) + \text{const}$. Also, if the heat capacity and thermal conductivity are both real values, q^2 becomes purely imaginary. Then, we can divide T_{ac} into real and imaginary parts to distinguish in-phase and out-of-phase oscillations of the temperature as follows [14,21];

$$\frac{l\pi\kappa}{P} T_{\text{ac}} = -\ln(qb) + \eta = -\frac{1}{2}\ln\left(\frac{2\omega b^2 C}{\kappa}\right) + \eta - \frac{\pi}{4}i \tag{3}$$

where η is a constant.

Finally, thermal quantities can be calculated from $V_{3\omega}$-the measured rms value of the 3ω voltage. $V_{3\omega} = V'_{3\omega} + iV''_{3\omega}$ is related to the temperature oscillation T_{ac} as

$$\begin{aligned} V_{3\omega} &= \frac{\omega}{2\pi} \int_0^{2\pi/\omega} I(t)R(t)\cos(3\omega t)dt \\ &= \frac{\omega}{2\pi} \int_0^{2\pi/\omega} 2I_0 \cos\omega t \left[R + \frac{dR}{dT} T_{\text{ac}} \cos(2\omega t)\right] \cos(3\omega t)dt \end{aligned}$$

$$= \frac{I_0 \alpha}{2} T_{ac}, \tag{4}$$

where α is the temperature coefficient of the resistance R of the heater and I_0 is the rms value of the electric current along the heater generating a power of $P = I_0^2 R$. Equation (3) can be rewritten in terms of $V'_{3\omega}$ as [22]

$$\kappa = -\frac{I_0^3 R \alpha}{4\pi \ell} \frac{d \ln \omega}{d V'_{3\omega}} \tag{5}$$

We consider now the case when a thin film with a lower thermal conductivity than the substrate, is located between the substrate and the strip. The increase in the temperature oscillation of the film ΔT_f can be expressed in terms of the thermal conductivity of the film κ_f [21]:

$$\Delta T_f = \frac{P t_f}{2 b \kappa_f} \tag{6}$$

where t_f is the film thickness.

3. EXPERIMENTAL

3.1. Sample Preparation

An As_2S_3 film of 1.0 μm thickness was coated on a slide glass for the measurement of transmittance change induced by photo-darkening. Then films of thickenesses of 0.5, 1.0, 2.0, and 4.0 μm were coated on a silicon wafer for the measurement of thermal conductivity. The uncertainty in the thickness was within $\pm 5\%$. All the films were coated in a thermal evaporator, and the thickness was monitored by the crystal oscillator. During the deposition, the coating rate was fixed at $5\,\text{nm}\cdot\text{s}^{-1}$.

3.2. Experiment

In order to investigate the photo-darkening effect, the fresh film coated on glass was irradiated for 10 min with the $100\,\text{mW}\cdot\text{cm}^{-2}$ Ar^+ laser beam whose wavelength is 514.5 nm. This photon energy (≈ 2.41 eV) is nearly consistent with the bandgap energy of As_2S_3 (≈ 2.34 eV). The transmittance of the irradiated film and fresh film was measured by the spectrophotometer in the wavelength range of 400–800 nm.

As shown in Fig. 3, a narrow gold metal strip and the rectangular pads are evaporated onto the sample through a stainless steel mask and the lead lines are electrically connected to the pads. The samples are

mounted in the sample holder using epoxy, and the lead lines are connected to the pads using silver paste. Then, the metal strip is connected by a four-probe type to the current and voltage lead lines. The width of the heater pattern is about 60 μm, and its length is 4 mm.

The measurement circuit is shown in Fig. 4 [22,23]. Since the ω component of the ac voltage at the heater causes a spurious signal at the lock-in amplifier, a Wheatstone bridge is used. R_1 and R_2 are fixed resistances, and R_v and R_s are the rheostat resistance and resistance of the gold pattern, respectively. Since R_2 and R_v are a few tens of kΩ and R_1 and R_s are a few tens of Ω, most of the current flows through R_1 and R_s. In the experimental apparatus, to balance the bridge circuit, we adjusted the value of R_v to suppress the signal of ω and separate out the 3ω component of the voltage signal. In order to prevent rapid temperature variation and to maintain a thermally stable state, the sample holder is put into a vacuum chamber whose temperature is controlled by the temperature controller between room temperature and 100 °C. Using a lock-in amplifier (SR 810 DSP), the amplitude and phase of the 3ω signal voltage were measured through the third harmonic mixer in the lock-in amplifier.

4. RESULTS AND DISCUSSION

Figure 5 shows the transmittance of fresh and irradiated film samples measured by the spectrophotometer. The transmittance of the light irradiated sample was reduced more than 10% and shifted toward the red wavelength of about 40 nm. This means that the normal photo-darkening, accompanied by the red shift of the absorption edge, was induced by the

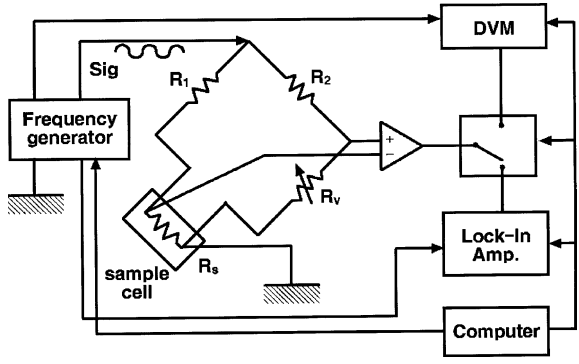

Fig. 4. Schematic of the apparatus for 3ω thermal conductivity measurements.

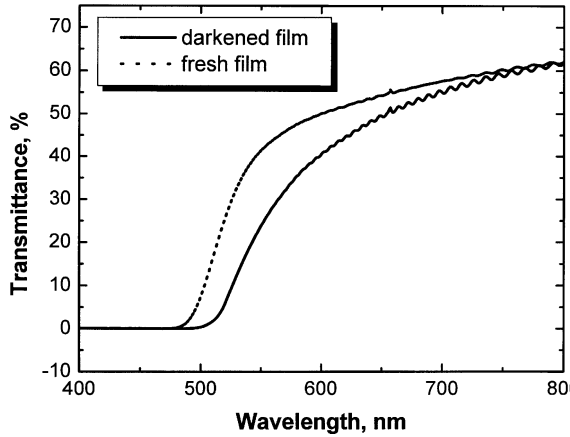

Fig. 5. Transmittance of the fresh and photo-darkened As_2S_3 films measured by spectrophotometer.

light absorption. It can be checked easily because the irradiated point was darkened.

Figures 6a, b, and c show the cross-sectional micrographs of fresh, photo-darkened, and annealed films, respectively. The annealing of the

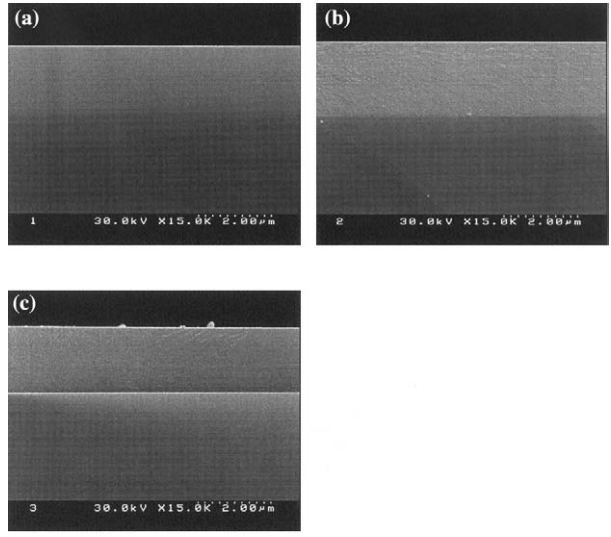

Fig. 6. Cross-sectional micrograph of (a) fresh film; (b) photo-darkened film; and (c) annealed film.

sample was performed at the glass transition temperature of 180°C for one hour. The grains in fresh films are small and uniform; however, the grain size becomes larger by the photo-darkening. After 1 h of annealing, the collected particles recovered nearly to the fresh film state; however, in some areas it did not fully recover to its original state. There are many reasons for this; however, we think the dominant source is the production of As_2O_3 by oxidation in air [1]. If the film was illuminated under vacuum conditions, the film could be restored completely. The stoichiometry and porosity of the film material which strongly affect the thermal conductivity must be checked more quantitatively.

In this experiment, it is necessary to know the variation of the resistance of the gold strip with temperature for measurement of the thermal conductivity. During the deposition of the gold strip, the TCR, defined as $(1dR)/(Rdt)$ was measured. The resistance could change for many other reasons such as an impurity; therefore, we measured and used them in the calculation [24].

If we assume that the silicon substrate and As_2S_3 film are thermally one-dimensionally connected, we can obtain the temperature variation of only the thin film by subtracting that of the substrate. In the case of a constant amplitude of the heater power per unit length, substituting this into the right side of Eq. (6), we can obtain the thermal conductivity of the thin film. For the case of a doped silicon substrate, we cannot neglect the electrical conductivity of the substrate; therefore, it is difficult to obtain an accurate TCR of the metal line directly. Consequently, we predicted the temperature variation of the substrate by simulation using the known thermal conductivity and diffusivity of silicon. The accuracy of this method was verified through the window glass, and it showed that the measured data and simulated data agree well within ±3% [24].

Figure 7a, b, and c shows the thermal conductivities of fresh, darkened, and annealed films, respectively, obtained with the 3ω method. We measured 5 times for each sample and the uncertainty was within ±6%. In all cases, as the temperature increases, the thermal conductivity also increases and at 100°C, it becomes nearly double the value at room temperature. This is a common phenomenon in amorphous materials because in such materials, the major heat conduction carrier involves phonons and as the temperature increases, its activation energy increases.

The results show that the thermal conductivity of fresh films was 0.14–0.27 $W \cdot m^{-1} \cdot K^{-1}$, increases to 0.28–0.47 $W \cdot m^{-1} K^{-1}$ after photo-darkening, and decreases to 0.19–0.42 $W \cdot m^{-1} \cdot K^{-1}$ after annealing of the sample. These changes can be explained by the change in microstructure produced from the photo-darkening and thermal annealing. As the previous photos in Fig. 6 show, the grain size becomes larger during the

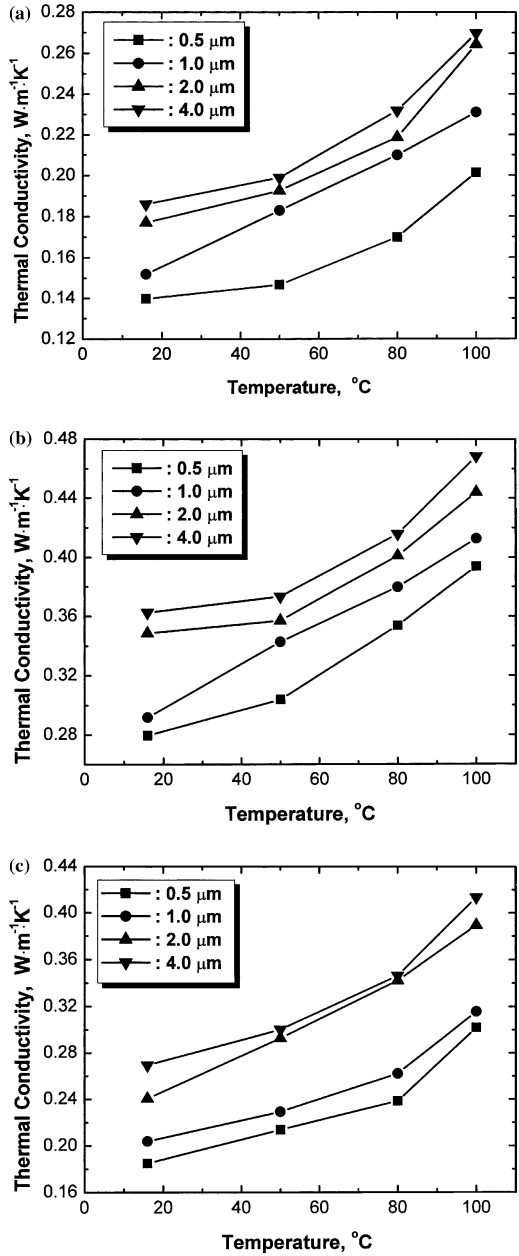

Fig. 7. Experimental thermal conductivity of (a) fresh films; (b) photo-darkened films; and (c) annealed films.

darkening. However, because of the oxidation, the film does not fully return to its original state after annealing.

This result is comparable to the literature values of several chalcogenide materials whose thermal conductivity is between 0.2 and 5.0 $W \cdot m^{-1} \cdot K^{-1}$ [14,25,26]. The important point is not the absolute value but the variation of the thermal conductivity. Table I shows the data obtained in this experiment.

The results also show that the thermal conductivity of thicker films are larger than for thinner films. This can be explained by the effect from the thermal resistances between the metal strip, film, and the surface of substrate. If we assume that these resistances exist, the obtained film thermal conductivity κ_f can be expressed as

$$\kappa_f = \frac{\kappa_i}{1 + R_i \kappa_i / t_f}, \tag{7}$$

where κ_i is the intrinsic thermal conductivity of the thin film independent of the thickness of the film and R_i is the total thermal resistance between the layers. From Eq. (7), we can see that the experimentally obtained thermal conductivity κ_f is always lower than κ_i and thinner films show lower κ_f than thicker films. Actually, because the thermal resistance R_i of the amorphous film is $2 \times 10^{-8} - 4 \times 10^{-8} m^2 \cdot K \cdot W^{-1}$ [27] depending on the thickness, the thermal conductivity changes about 20% at maximum. However, the result shows that the changing rate is larger than this; therefore, additional investigations will be required.

5. CONCLUSIONS

The thermal conductivity of As_2S_3 films, for which a knowledge of their thermal properties is insufficient compared to optical and electrical properties, was measured by the 3ω method. The fresh, photo-darkened, and annealed As_2S_3 thin films coated on a silicon wafer, whose thicknesses are 0.5, 1.0, 2.0, and 4.0 μm, were measured in the range from room temperature to 100 °C. Because thermal resistance between the layers increases, the measured thermal conductivity of thinner films decreases. The results also show that the thermal conductivities of fresh films were 0.14–0.27 $W \cdot m^{-1} \cdot K^{-1}$, increasing to 0.28–0.47 $W \cdot m^{-1} \cdot K^{-1}$ after the illumination of light on the sample, and decreasing to 0.19–0.42 $W \cdot m^{-1} \cdot K^{-1}$ after annealing of the sample. This can be explained by the change of microstructure produced from the photo-darkening and thermal annealing.

In order to understand the mechanism for the change of thermal conductivity in more detail, the investigation must be repeated for a wide variety of samples whose illumination time and stoichiometry of the coated

Table I. Experimental Thermal Conductivities of As_2S_3 Thin Films

Temp. (°C)	Thermal Conductivity ($W \cdot m^{-1} \cdot K^{-1}$)											
	Fresh Films				Darkened Films				Annealed Films			
	0.5 μm	1.0 μm	2.0 μm	4.0 μm	0.5 μm	1.0 μm	2.0 μm	4.0 μm	0.5 μm	1.0 μm	2.0 μm	4.0 μm
23	0.139	0.152	0.177	0.186	0.280	0.292	0.349	0.363	0.185	0.204	0.241	0.269
50	0.147	0.183	0.193	0.199	0.304	0.343	0.357	0.373	0.214	0.229	0.293	0.300
80	0.167	0.210	0.212	0.232	0.354	3.797	0.401	0.416	0.238	0.262	0.342	0.346
100	0.201	0.231	0.264	0.270	0.394	0.413	0.444	0.468	0.302	0.316	0.390	0.414

film must be analyzed. We expect that our experimental results can be the baseline data for the application of chalcogenides to imaging, holography, and optical memories which utilize the change of thermal properties.

ACKNOWLEDGMENT

This work was supported by 2002 Research Fund of University of Ulsan.

REFERENCES

1. S. A. Keneman, *Appl. Phys. Lett*. **19**:205 (1971).
2. J. P. De Neufville, S. C. Moss, and S. R. Ovshinsky, *J. Non-Cryst. Solids* **13**:191 (1974).
3. K. Tanaka and Y. Ohtsuka, *J. Appl. Phys.* **49**:6132 (1978).
4. O. Nordam, N. Nordam, and J. Teteris, *Opt. Commun*. **146**:69 (1998).
5. S. D. Sartale and C. D. Lokhande, *Mater. Res. Bull*. **35**:1345 (2000).
6. K. Tanaka, *J. Non-Cryst. Solids* **35 & 36**:1023 (1980).
7. A. Ganjoo, K. Shimakawa, K. Kitano, and E. A. Davis, *J. Non-Cryst. Solids* **299–302**:917 (2002).
8. S. R. Elliott, *J. Non-Cryst. Solids* **81**:71 (1986).
9. S. C. Agarwal and H. Fritzsche , *Phys. Rev*. **B10**:4351 (1974).
10. B. Meyer, *Chem. Rev.* **76**:367 (1976).
11. M. Frumar, A. P. Firth, and A. E. Owen, *J. Non-Cryst. Solids* **192 & 193**:447 (1995).
12. S. D. Sartale and C. D. Lokhande, *Mater. Res. Bull.* **35**:1345 (2000).
13. A. Zakery, P. J. S. Ewen, and A. E. Owen, *J. Non-Cryst. Solids* **198–200**:769 (1996).
14. D. G. Cahill and R. O. Pohl, *Phys. Rev*. **B35**:4067 (1987).
15. D. G. Cahill, Rev. *Sci. Instrun*. **61**:802 (1990).
16. D. G. Cahill, M. Katiyer, and J. R. Abelson, *Phys. Rev*. **B50**:6077 (1994).
17. S. M. Lee and D. G. Cahill, *Phys. Rev*. **B52**:253 (1995).
18. R. Street, *Sol. Stat. Commun*. **24**:363 (1977).
19. H. S. Carslow and J. C. Jaeger, Conduction of Heat in Solids (Oxford University Press, Oxford, 1959), p. 193.
20. Y. H. Jeong, Thermochim. Acta **304/305**:67 (1997).
21. S. M. Lee and D. G. Cahill, J. Appl. Phys. **8**:2590 (1997).
22. D. J. Kim, D. S. Kim, C. Cho, S. W. Kim, S. H. Lee, and J. C. Kim, Int. J. Thermophys. **25**:281 (2004).
23. Y. H. Jeong, D. J. Bae, T. W. Kwon, and I. K. Moon, *J. Appl. Phys*. **70**:6166 (1991).
24. B. R. Park, D. J. Seong, J. C. Kim, S. W. Kim, and S. H. Hahn, *Ungyong Mulli* **10**: 530 (1997).
25. M. A. Pepescu, *Non-Crystalline Calcogenides* (Kluwer Academic Publishers, Dordrecht, 2000), pp. 315–320.
26. R. Wawryk, Cz. Marcucha, K. Balcerek, B. M. Terzijska, and Z. G. Ivanova, *Cryogenics* **4**:749 (2000).
27. T. Yamane, N. Nagai, S. Katayama, and M. Todoki, *J. Appl. Phys*. **91**:9772 (2002).